JOC Article
pubs.acs.org/joc

Expanding the Cavity Size: Preparation of 2:1 Inclusion Complexes Based on Dinuclear Square Metallocycles

Víctor Blanco, Albert Gutiérrez,[†] Carlos Platas-Iglesias, Carlos Peinador,* and José M. Quintela*

Departamento de Química Fundamental, Facultad de Ciencias, Universidade da Coruña, Campus A Zapateira, 15071, A Coruña, Spain. [†]Current address: Departament de Química Inorgànica, Universitat de Barcelona, c/Martí i Franquès 1-11, 08028 Barcelona, Spain.

capeveqo@udc.es

Received May 18, 2009

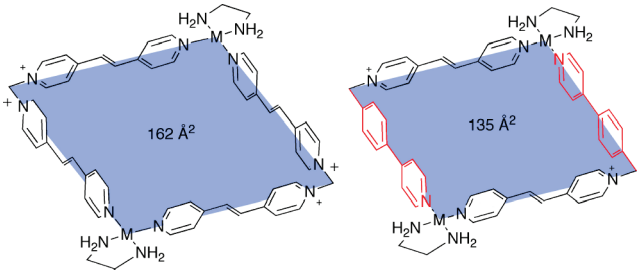

The self-assembly of two new ligands based on the *trans*-1,2-bis(4-pyridyl)ethylene motif with palladium or platinum complexes led to quadrangular metallocycles. 1,1′-Methylenebis(4-((*E*)-2-(pyridin-4-yl)vinyl)pyridinium gave the square metallocycles, while the second ligand, which is less symmetrical, gave a mixture of the regioisomeric metallocyles. The metallocycles display the ideal disposition of the π-acceptor units to maximize the π-stacking interactions with aromatic guests. Thus, molecular recognition of π-donor aromatic guests by square metallocycles produced the corresponding 2:1 inclusion complexes. On the other hand, starting from the mixture of regioisomers, the *incorrect* regioisomer rearranged to the *correct* metallocycle upon the addition of aromatic guests. On the basis of this behavior, a [3]catenane was obtained regioselectively from the mixture of the regioisomeric metallocycles and the appropriate cyclophane. The formation of this catenane was confirmed by NMR and X-ray crystallographic studies.

Introduction

The utilization of transition metal centers and dative bond for directing the formation of two- and three-dimensional supramolecular structures has proved to be a highly convenient self-assembly strategy.[1] On the basis of this methodology, a myriad of polygonal metallomacrocyles such as triangles, squares, pentagons, hexagons, and molecular cages have been reported in the last decades.[2] Thus, the shape of the molecular polygon is predetermined by the

(1) (a) Swiegers, G. F.; Malefetse, T. J. *Chem. Rev.* **2000**, *100*, 3483. (b) Fujita, M.; Tominaga, M.; Hori, A.; Therrien, B. *Acc. Chem. Res.* **2005**, *38*, 369. (c) Dinolfo, P. H.; Hupp, J. T. *Chem. Mater.* **2001**, *13*, 3113. (d) Caulder, D. L.; Raymond, K. N. *J. Chem. Soc., Dalton Trans.* **1999**, 1185. (e) Steel, P. J. *Acc. Chem. Res.* **2005**, *38*, 243. (f) Leininger, S.; Olenyuk, B.; Stang, P. J. *Chem. Rev.* **2000**, *100*, 853. (g) Würthner, F.; You, C.-C.; Saha-Möller, C. R. *Chem. Soc. Rev.* **2004**, 133. (h) Collin, J.-P.; Heitz, V.; Bonnet, S.; Sauvage, J.-P. *Inorg. Chem. Commun.* **2005**, *8*, 1063. (i) Holliday, B. J.; Mirkin, C. A. *Angew. Chem., Int. Ed.* **2001**, *40*, 2022. (j) Cotton, F. A.; Lin, C.; Murillo, C. A. *Acc. Chem. Res.* **2001**, *34*, 759. (k) Fujita, M. *Chem. Soc. Rev.* **1998**, *27*, 417.

(2) (a) Tárkányi, G.; Jude, H.; Pálinkás, G.; Stang, P. J. *Org. Lett.* **2005**, *7*, 4971. (b) Janzen, D. E.; Patel, K. N.; VanDerveer, D. G.; Grant, G. J. *Chem. Commun.* **2006**, 3540. (c) Wu, Z.-Q.; Jiang, X.-K.; Li, Z.-T. *Tetrahedron Lett.* **2005**, *46*, 8067. (d) Campos-Fernández, C. S.; Schottel, B. L.; Chifotides, H. T.; Bera, J. K.; Bacsa, J.; Koomen, J. M.; Russell, D. H.; Dunbar, K. R. *J. Am. Chem. Soc.* **2005**, *127*, 12909. (e) Jiang, H.; Lin, W. *J. Am. Chem. Soc.* **2003**, *125*, 8084. (f) Cho, Y. L.; Uh, H.; Chang, S.-Y.; Chang, H.-Y.; Choi, M.-G.; Shin, I.; Jeong, K.-S. *J. Am. Chem. Soc.* **2001**, *123*, 1258. (g) O'donnell, J. L.; Zuo, X. B.; Goshe, A. J.; Sarkisov, L.; Snurr, R. Q.; Hupp, J. T.; Tiede, D. M. *J. Am. Chem. Soc.* **2007**, *129*, 1578. (h) Burchell, T. J.; Puddephatt, R. J. *Inorg. Chem.* **2005**, *44*, 3718. (i) Cotton, F. A.; Lin, C.; Murillo, C. A. *Inorg. Chem.* **2001**, *40*, 478. (j) Stulz, E.; Scott, S. M.; Bond, A. D.; Teat, S. J.; Sanders, J. K. M. *Chem.—Eur. J.* **2003**, *24*, 6039. (k) Zhao, L.; Northrop, B. H.; Stang, P. J. *J. Am. Chem. Soc.* **2008**, *130*, 11886. (l) Suzuki, K.; Iida, J.; Sato, S.; Kawano, M.; Fujita, M. *Angew. Chem., Int. Ed.* **2008**, *47*, 5780. (m) Zhao, L.; Northrop, B. H.; Zheng, Y. R.; Yang, H. B.; Lee, H. J.; Lee, Y. M.; Park, J. Y.; Chi, K. W.; Stang, P. J. *J. Org. Chem.* **2008**, *73*, 6580. (n) Ferrer, M.; Gutiérrez, A.; Mounir, M.; Rossell, O.; Ruiz, E.; Rang, A.; Engeser, M. *Inorg. Chem.* **2007**, *46*, 3395.

DOI: 10.1021/jo901034c Published on Web 08/10/2009

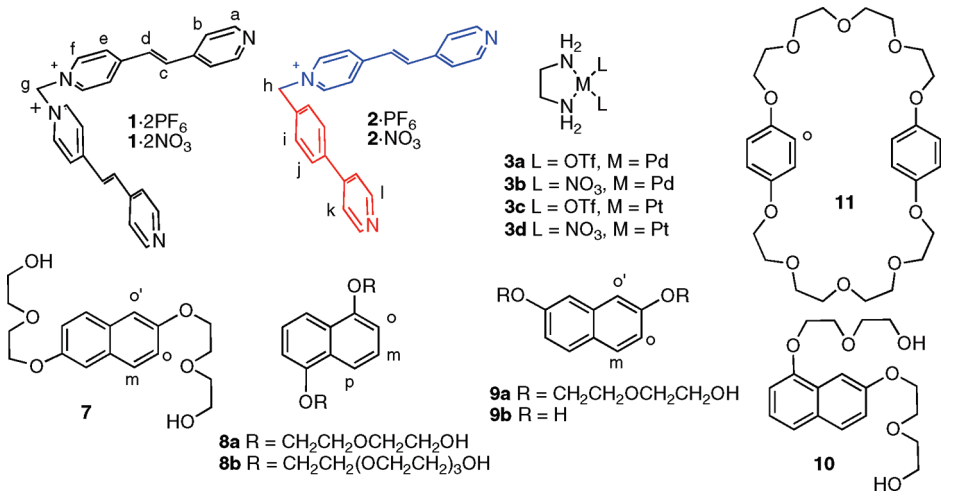

FIGURE 1. Structures used in this work.

choice of the metal center and ligand geometries that direct the self-assembly process. The success of the metal-directed self-assembly approach is mainly due to two reasons: (i) The access to bond angles unavailable in carbon chemistry and (ii) a wide range of kinetic lability of the metal−heteroatom bond, which allows the correction of defect products by selecting appropriate reaction conditions.

The interactions between aromatic rings control a vast and fascinating variety of phenomena such as the stabilization of the DNA double helix,[3] the tertiary structure of proteins,[4] crystal packing of aromatic molecules,[5] and columnar structures of discotic liquid crystals.[6] In discrete supramolecular systems, $\pi-\pi$ interactions have been widely utilized to synthesize many host−guest complexes[7] and other assemblies such as catenanes and rotaxanes.[8]

In the last years, our group has reported several molecular rectangles and squares based on the self-assembly of *N*-monoalkylated 4,4′-bipyridine ligands and square-planar metal centers. In most cases the dimensions and shape of the cavity defined by squares or rectangles, as well as the π-deficient character of the ligand, allowed the insertion of aromatic guests into the metallocycle. The complexes are stabilized by means of a combination of π-stacking, hydrogen bonding, and hydrophobic forces. Therefore, the correct angles at the metal center, the length of the side defined by the ligand, and its π-complementary character determine the ability of metallocycles to act as receptors. Taking advantage of these characteristics, we have recently reported the self-assembly of inclusion complexes with 1:1 and 2:1 stoichiometry and [2]- and [3]catenanes.[9]

In this paper we present two new quadrangular metallocycles with elongated sides based on a *trans*-1,2-bis(4-pyridyl)ethylene motif. Thus, these longer sides could potentially provide metallocycles with larger cavities, and eventually with enhanced selectivity toward larger guests. Both metallocycles would have an ideal distance between opposite sides to bind two aromatic rings in the cavity, so the formation of 2:1 inclusion complexes and [3]catenanes should be expected.

Results and Discussion

Molecular components used in this work are depicted in Figure 1. Ligands **1**·2PF_6 and **2**·PF_6 were synthesized by *N*-alkylation of *trans*-1,2-bis(4-pyridyl)ethylene with dibromomethane and 4-(4-chloromethylphenyl)pyridine, respectively. Both hexafluorophosphate salts can be converted into the corresponding water-soluble nitrates with tetrabutylammonium nitrate. It is worthy of note that **1**·2PF_6 proved to be more resistant to thermal decomposition than its 4,4′-bipyridine analogue.[9a] No decomposition was detected by ^{1}H NMR after heating a CD_3CN solution of the ligand at 75 °C for 2 d.

Addition of 1 equiv of (en)Pd(NO_3)$_2$ to a solution of ligand **1**·2NO_3 (10 mM in D_2O) at room temperature resulted in the expected formation of the square metallocycle **4a** (Figure 2) as can be seen from inspection of the 1D and 2D NMR data. Similar results were obtained in CD_3CN solutions upon the self-assembly of (en)Pd(OTf)$_2$ and **1**·2PF_6. The ^{1}H NMR spectrum of metallocycle **4a** in CD_3CN showed the characteristic downfield shifts of protons H_a and H_b due to the coordination of the pyridine ring to the Pd center. The ^{1}H NMR spectra in both solvents are compatible with the

(3) (a) Hunter, C. A.; Sanders, J. K. M. *J. Am. Chem. Soc.* **1990**, *112*, 5525. (b) Saenger, W. *Principles of Nucleic Acid Structure*; Springer-Verlag: New York, 1984. (c) Kool, E. T. *Chem. Rev.* **1997**, *97*, 1473.

(4) (a) Burley, S. K.; Petsko, G. A. *Science* **1985**, *229*, 23. (b) Hunter, C. A.; Singh, J.; Thornton, J. M. *J. Mol. Biol.* **1991**, *218*, 837.

(5) (a) Anderson, H. L.; Bashall, A.; Henrick, K.; McPartlin, M.; Sanders, J. K. M. *Angew. Chem., Int. Ed. Engl.* **1994**, *33*, 429. (b) Martin, C. B.; Patrick, O.; Cammers-Goodwin, A. *J. Org. Chem.* **1999**, *64*, 7568.

(6) (a) Bushby, R. J.; Lozman, O. R. *Curr. Opin. Colloid Interface Sci.* **2002**, *7*, 343.

(7) (a) Sygula, A.; Fronczek, F. R.; Sygula, R.; Rabideau, P. W.; Olmstead, M. M. *J. Am. Chem. Soc.* **2007**, *129*, 3842. (b) Yoshizawa, M.; Nakagawa, J.; Kurnazawa, K.; Nagao, M.; Kawano, M.; Ozeki, T.; Fujita, M. *Angew. Chem., Int. Ed.* **2005**, *44*, 1810.

(8) (a) *Molecular Catenanes, Rotaxanes and Knots*; Sauvage, J.-P., Dietrich- Buchecker, C., Eds.; Wiley-VCH: Weinheim, Germany, 1999. (b) Amabilino, D. B.; Stoddart, J. F. *Chem. Rev.* **1995**, *95*, 2725. (c) Badjic, J. D.; Ronconi, C. M.; Stoddart, J. F.; Balzani, V.; Silvi, S.; Credi, A. *J. Am. Chem. Soc.* **2006**, *128*, 1489. (d) Payer, D.; Rauschenbach, S.; Malinowski, N.; Konuma, M.; Virojanadara, C.; Starke, U.; Dietrich-Buchecker, C.; Collin, J. P.; Sauvage, J. P.; Lin, N.; Kern, K. *J. Am. Chem. Soc.* **2007**, *129*, 15662.

(9) (a) Blanco, V.; Chas, M.; Abella, D.; Peinador, C.; Quintela, J. M. *J. Am. Chem. Soc.* **2007**, *129*, 13978. (b) Chas, M.; Blanco, V.; Peinador, C.; Quintela, J. M. *Org. Lett.* **2007**, *9*, 675. (c) Chas, M.; Pía, E.; Toba, R.; Peinador, C.; Quintela, J. M. *Inorg. Chem.* **2006**, *45*, 6117. (d) Abella, D.; Blanco, V.; Pía, E.; Chas, M.; Platas-Iglesias, C.; Peinador, C.; Quintela, J. M. *Chem. Commun.* **2008**, 2879. (e) Peinador, C.; Blanco, V.; Quintela, J. M. *J. Am. Chem. Soc.* **2009**, *131*, 920.

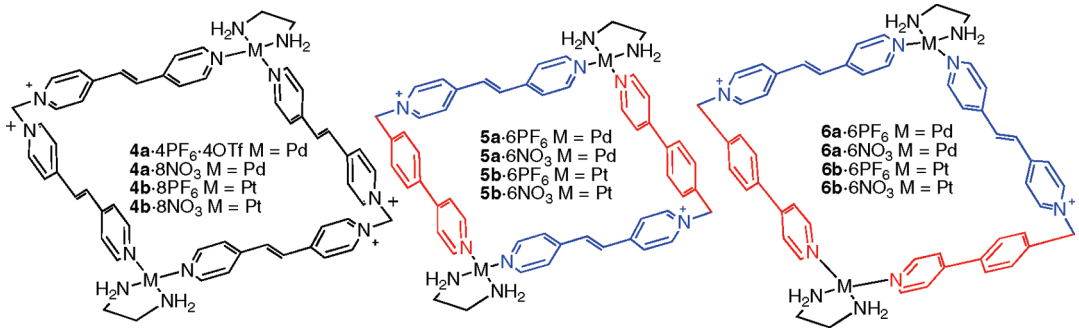

FIGURE 2. Structures of metallocycles **4**−**6**.

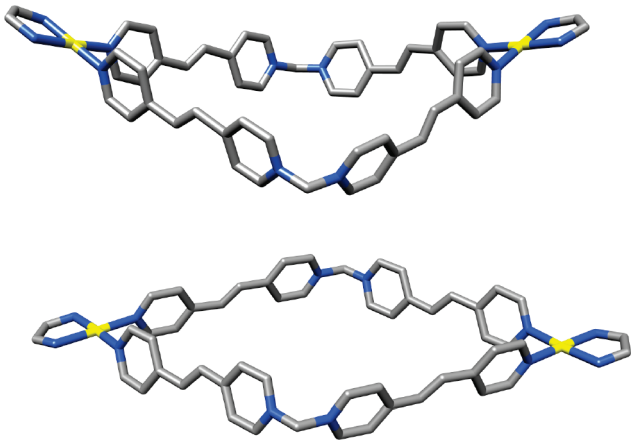

FIGURE 3. Solid-state structures of the puckered (top) and flat (bottom) conformers of **4a**·4OTf·4PF_6.

presence of either a single compound or two or more species that are in fast equilibrium on the ^{1}H NMR time scale. We carried out dilution studies to support the presence of the metallocycle **4a** as a single species in solution. The spectra remain unchanged in the 5.0−1.25 mM (CD_3CN) and 5.0−0.25 mM (D_2O) concentration range. Above these limits, new resonances appear, which can be attributed to some kind of aggregation.

Single crystals of metallocycle **4a**·4OTf·4PF_6 were obtained from a solution of ligand **1**·2PF_6 and (en)Pd(OTf)$_2$ in acetonitrile. Unfortunately, the crystals were of limited quality and the resulting data are somewhat poor due to a triflate counterion that is disordered, although the unambiguous assignment of the metallocycle moiety was possible. The crystal structure shows the presence of two conformers of metallocycle **4a** with a rhombic cavity (Figure 3).

In one conformer one corner of the rhomboid is out of plane, with the metallocycle showing a puckered conformation, with the angles between planes being 49° and 39° for the two planes defined by $PtCH_2Pt$ corners and the two planes defined by CH_2PtCH_2, respectively. The second conformer present in the crystal is centrosymmetric with a planar disposition of the four corners of the metallocycle. The Pd atoms show a square-planar coordination environment with Pd−N(pyridine) bond distances ranging between 2.018 and 2.056 Å. The NCN angles at the methylene corners are 111° and 109° in the puckered and the planar conformers, respectively. The angles at the Pd corners of N(Py)PdN(Py) amount to 89° and 92° in the angular conformer and 88° in the planar one. The diagonals measured in the centrosymmetric conformer are 14.3 (distance between methylene groups) and 21.1 Å (distance between Pd atoms), while those in the puckered isomer amount to 15.2 and 19.2 Å, respectively.

Platinum metallocycle **4b**·8PF_6 was synthesized in 65% yield by the thermodynamically driven self-assembly reaction at 70 °C to take advantage of the "molecular lock" strategy. The NMR data showed spectroscopic characteristics very similar to the corresponding palladium analogue. The HRMS-ESI supported the proposed structure showing m/z values and isotopic pattern distributions in excellent agreement with the calculated ones (see the Supporting Information). The platinum macrocycle could also be isolated as its nitrate salt **4b**·8NO_3 by adding an excess of tetrabutylammonium nitrate to an acetonitrile solution of **4b**·8PF_6.

In a previous work, we reported the formation of 2:1 inclusion complexes between aromatic guests and a square metallocycle with 4,4′-bipyridine sides.[10] Although the introduction of the double bond between the bipyridine units in ligand **1**·2PF_6 extends slightly the sides of the metallocycle, we expected that this metallocycle could also lead to the formation of 2:1 inclusion complexes. Indeed, the self-assembly of ligand **1**·2PF_6, (en)Pd(OTf)$_2$, and compounds **7** or **9a** in CD_3CN produced changes in their ^{1}H NMR spectra that are consistent with the formation of the corresponding inclusion complexes, as the signals due to aromatic protons of the naphthalene units shifted to shorter frequencies (averaged shift: $\Delta\delta = -0.15$ ppm). However, the chemical shifts of the metallocycle protons were hardly affected. This fact can be ascribed to two opposite effects, as the pyridine units parallel to the naphthalene units are expected to experience a shielding effect, while the pyridine units orthogonal to the guests are deshielded due to [C−H···π] interactions. Because the complexation−decomplexation process is fast in the NMR time scale, the signals for the orthogonal and parallel pyridines are averaged and the two effects are mutually canceled.

On the contrary, the addition of 2 equiv of substrate **8a** to a 5 mM solution of **4a**·4OTf·4PF_6 in acetonitrile resulted in a color change from intense blue to green. However, the ^{1}H NMR spectrum did not reveal significant changes in the chemical shifts of the free components.

The complexation process was also studied in aqueous solution. In this solvent the hydrophobic forces and

(10) Blanco, V.; Chas, M.; Abella, D.; Pía, E.; Platas-Iglesias, C.; Peinador, C.; Quintela, J. M. *Org. Lett.* **2008**, *10*, 409.

TABLE 1. Selected ^{1}H and ^{13}C NMR Chemical Shift Data ($\Delta\delta$) for Inclusion Complexes in D_2O and [3]Catenane $12\cdot6PF_6$ (5 mM in CD_3CN)[a]

		metallocycle protons[b]					guest protons[c]			
compd		b	c	d	k	l	o	o′	m	p
$(\mathbf{7})_2\mathbf{4a}\cdot8NO_3$		0.00	0.00	−0.02			−0.32	−0.19	−0.54	
$(\mathbf{8a})_2\mathbf{4a}\cdot8NO_3$		0.00	−0.04	−0.08			−0.20		−0.23	−0.27
$(\mathbf{8b})_2\mathbf{4a}\cdot8NO_3$		0.00	−0.04	−0.06			−0.13		−0.13	−0.14
$(\mathbf{9a})_2\mathbf{4a}\cdot8NO_3$		−0.04	−0.17	−0.22			−0.24	−0.21	−0.25	
$(\mathbf{9b})_2\mathbf{4a}\cdot8NO_3$		−0.03	−0.09	−0.10			−0.21	−0.16	−0.17	
$(\mathbf{8a})_2\mathbf{5a}\cdot6NO_3$	H	−0.37	−1.06	−1.24	0.4	0.35	—[d]		—[d]	—[d]
	C	−0.2	−1.8	−1.7	−0.3	0.2	—[d]		—[d]	—[d]
$(\mathbf{9a})_2\mathbf{5a}\cdot6NO_3$	H	−0.43	−1.15	−1.3	0.27	0.31	−0.45	−0.68	−0.73	
	C	−0.3	−1.4	−1.9	0.1	0.1	−0.5	0.0	−0.7	
$(\mathbf{10})_2\mathbf{5a}\cdot6NO_3$	H	−0.49	−1.3	−1.45	0.32	0.32				
	C	−0.3	−2.2	−2.3	0.1	0.1				
$\mathbf{12}\cdot6PF_6$	H	−0.66	−1.16	−1.19	0.1	0.19	−0.96			
	C	−1.9	−2.8	−2.7	0.4	0.4	−1.3			

[a]Hydrogen and carbon labels are defined in Figure 1. [b]The δ values are compared to those of the corresponding free metallocycle ($\mathbf{4a}\cdot8NO_3$, $\mathbf{5a}\cdot6NO_3$). [c]The δ values are compared to those of the corresponding free guest (**7**−**10**). [d]Not determined because of line broadening.

π-stacking should favor the insertion of the aromatic guests into the cavity of the metallocycle.[11] Thus, the addition of 2 equiv of **8a** to a 1 mM solution of $\mathbf{4a}\cdot8NO_3$ and sonication for 2 h changed the color of the solution from pale red to intense red. The ^{1}H NMR spectra of the inclusion complexes $(\mathbf{7})_2\mathbf{4a}\cdot8NO_3$, $(\mathbf{8a})_2\mathbf{4a}\cdot8NO_3$, and $(\mathbf{9a})_2\mathbf{4a}\cdot8NO_3$ exhibited larger upfield shifts for the aromatic protons of the guests than in acetonitrile solution (Table 1). The same color changes and chemical shift tendencies were observed upon sonication for the corresponding platinum inclusion complexes. The continuous variation method (Job plot) confirmed the stoichiometry of complex formation in solution between **9a** and metallocycle $\mathbf{4b}\cdot8NO_3$ to be 2:1 (guest:host) (Figure 4).[12] The UV−vis titrations method was used to determine association constants in aqueous media for the inclusion complexes $(\mathbf{8b})_2\mathbf{4a}\cdot8NO_3$, $(\mathbf{9a})_2\mathbf{4a}\cdot8NO_3$, and $(\mathbf{9b})_2\mathbf{4a}\cdot8NO_3$ (K_a = 478 ± 84, 315 ± 89, and 120 ± 23, respectively).[13] All of the titration curves were well fitted to the 2:1 binding model.[14]

Surprisingly, the self-assembly of ligand $\mathbf{2}\cdot NO_3$ and palladium complex **3b** in D_2O led to a mixture of two species in a 1:1 ratio, which were assigned as the two 2 + 2 isomeric metallocycles $\mathbf{5a}\cdot6NO_3$ and $\mathbf{6a}\cdot6NO_3$ (Figure 2). The hexafluorophosphate salts of **5a** and **6a** could be precipitated from the corresponding nitrates by addition of potassium hexafluorophosphate. The NMR spectra recorded upon redissolution of the solid in CD_3CN indicated that both isomeric metallocycles persist in solution with a 1:1 ratio. The ^{1}H NMR spectra of the mixture of **5a**,**6a** remained unaltered upon dilution (concentration range 2.5−0.25 and 5.0−0.25 mM in D_2O and CD_3CN, respectively). In addition, the DOSY experiments provided very similar diffusion coefficients for the two species. These results indicate that the two species present in solution have a very similar size, in agreement with the proposed structures. Similar results were obtained from the self-assembly of the platinum complexes.

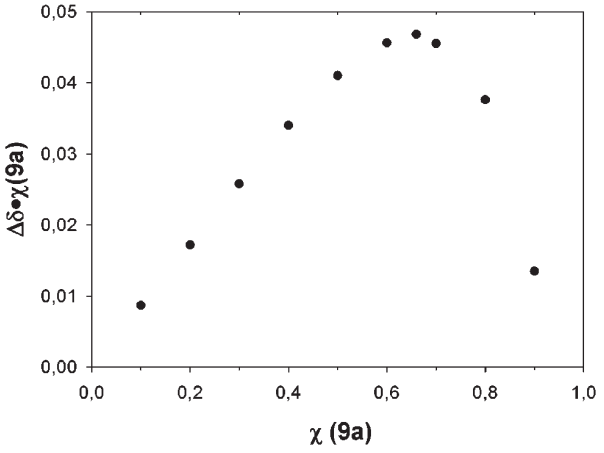

FIGURE 4. Job plot showing the 2:1 (H:G) stoichiometry of a complex formed between guest **9a** and $\mathbf{4b}\cdot8NO_3$ (total concentration 2 mM). The induced change in the chemical shift of $H_{o'}$ is plotted versus the molar fraction of **9a**.

Mass spectrometry supported the structure of the square metallocycles. The HRMS-ESI spectrum of the platinum analogues **5b**,**6b** showed peaks resulting from the loss of three to six hexafluorophosphate anions.

Aiming to obtain information on the solution structure of the **5a**,**6a** metallocycles, these systems were characterized by means of DFT calculations (B3LYP model).[15,16] In these calculations the 6-31G(d) basis set was used for the ligand atoms, while for Pd atoms the effective core potential of Wadt and Hay (Los Alamos ECP) included in the LanL2DZ basis set was applied.[17] Our calculations provide two minimum energy conformations with nearly undistorted C_2 symmetries (Figure 5).[18] These minimum energy conformations correspond to two isomeric rhombic metallocycles that differ in the relative arrangement of the two ligands. Indeed, in **5a** each Pd^{II} ion is coordinated by a 4-phenylpyridine and a 4-vinylpyridine unit, while in **6a** one of the Pd^{II} ions is coordinated to two 4-phenylpyridine moieties, and the

(11) (a) Smithrud, F.; Diederich, F. *J. Am. Chem. Soc.* **1990**, *112*, 339. (b) Ferguson, S. B.; Sanford, E. M.; Seward, E. M.; Diederich, F. *J. Am. Chem. Soc.* **1991**, *113*, 5410. (c) Cubberley, M. S.; Iverson, B. L. *J. Am. Chem. Soc.* **2001**, *123*, 7560.

(12) Job, P. *Ann. Chim.* **1928**, *9*, 113.

(13) (a) Connors, K. A. *Binding Constants*; Wiley: New York, 1987. (b) Schneider, H.-J.; Yatsimirsky, A. K. *Principles and Methods in Supramolecular Chemistry*; John Wiley & Sons: New York, 2000.

(14) Compouds **7**, **8a**, and **10** are sparingly soluble in water and the determination of their binding constants was not possible.

(15) Becke, A. D. *J. Chem. Phys.* **1993**, *98*, 5648.

(16) Lee, C.; Yang, W.; Parr, R. G. *Phys. Rev. B* **1988**, *37*, 785.

(17) Hay, P. J.; Wadt, W. R. *J. Chem. Phys.* **1985**, *82*, 270.

(18) The stationary points found on the potential energy surfaces as a result of the geometry optimizations have been tested to represent energy minima rather than saddle points via frequency analysis.

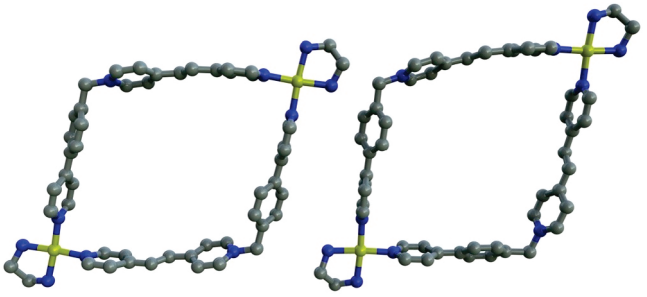

FIGURE 5. Calculated structures of metallocycles **5a** (left) and **6a** (right).

second metal is coordinated by two 4-vinylpyridine ones. Both **5a** and **6a** possess similar cavity dimensions, with Pd···Pd distances of ca. 18.8 Å, and $CH_2\cdots CH_2$ distances of ca. 14.5 Å. In **5a** the C_2 symmetry axis is perpendicular to the plane described by the four vertexes of the rhombic cavity defined by the two Pd atoms and the two methylenic carbon atoms. On the contrary, in **6a** the C_2 symmetry axis contains the two Pd atoms. Thus, the two minimum energy conformations obtained from our DFT calculations show the same symmetry properties, and therefore they are expected to provide very similar NMR spectral patterns. Our calculations predict a small energy difference between **5a** and **6a**, the in vacuo relative free energy, $\Delta G°_{298K} = G°_{\mathbf{5a}} - G°_{\mathbf{6a}}$, amounting to -0.54 kcal·mol^{-1}.[19] These results are in line with the formation of both **5a** and **6a** in solution with nearly identical populations.

Addition of guests **8**−**10** to a solution of **5a**,**6a**·$6NO_3$ in D_2O resulted in the total reorganization of the *incorrect* metallocycle **6a**·$6NO_3$. Most likely, the reorganization of the system toward one species is driven by the $\pi-\pi$ stacking interactions and facilitated by the kinetic lability of Pd−N bonds. Indeed, metallocycle **6a**·$6NO_3$ does not display the correct disposition of the aromatic systems to maximize the $\pi-\pi$ stacking interactions, as the better π-acceptor di(pyridin-4-yl)ethene systems are in adjacent sides. Furthermore, the opposite sides of rhomboid **6a**·$6NO_3$ are not parallel, as shown by the DFT calculated structure (Figure 5). The ^{1}H NMR spectra are compatible with the presence of the inclusion complexes of the metallocycle **5a**·$6NO_3$. Thus, the protons of the di(pyridin-4-yl)ethene sides are shielded (H_b, H_c, and H_d, see Table 1) while those of the phenylpyridine side are deshielded (H_k and H_l). This tendency is consistent with previously reported findings,[10] and suggests that the phenylpyridine units are involved in [C−H···π] interactions with the aromatic protons of the guests.

It is interesting to note that larger or smaller aromatic guests such as pyrene or hydroquinone do not interact with metallocycles **4a**·$8NO_3$ and **5a**,**6a**·$6NO_3$. Thus, the extra length provided by the double bond is not enough to allow the inclusion of pyrene, but it extends the distance between opposite sides of the cavity, which weakens the interaction with hydroquinone. Thus, it is reasonable to conclude that the naphthalene derivatives **7**−**10** have the appropriate size for their inclusion in metallocycles **4a**·$8NO_3$ and **5a**,**6a**·$6NO_3$.

(19) Relative free energies include zero point energy corrections and thermal terms obtained from frequency analyses.

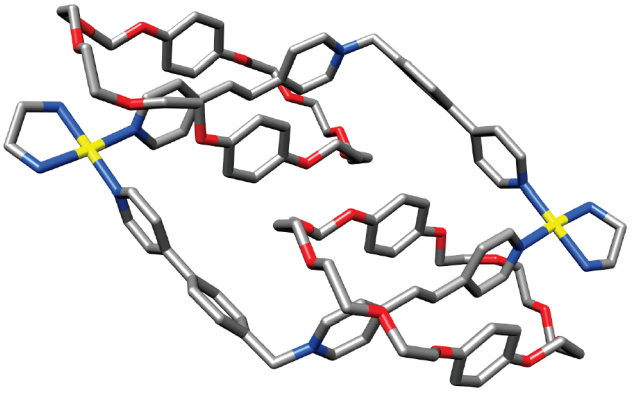

FIGURE 6. Crystal structure of catenane **12**·$6PF_6$. The color labeling scheme is as follows: nitrogen (blue), oxygen (red), palladium (yellow), and carbon (gray). Solvent molecules, hydrogen atoms, and counterions have been omitted for clarity.

Finally, metallocycles **5a**,**6a** provide a new example of regioselective catenation as a result of the template directed reorganization described above.[20] It was necessary to add 10 equiv of cyclophane **11** (Figure 1) to a solution (5 mM) of metallocycles **5a**,**6a**·$6PF_6$ in CD_3CN to achieve the reorganization to the single [3]catenane **12**·$6PF_6$. The ^{1}H NMR spectrum of **12**·$6PF_6$ shows that the exchange between the "inside" and "alongside" hydroquinol rings in the [3]catenane is fast at room temperature, resulting in an averaged signal (δ = 5.71 ppm) for the aromatic protons of **11**. The diffusion coefficients of catenane **12**·$6PF_6$ and metallocycles **5a**,**b**·$6PF_6$ obtained from DOSY experiments showed that the catenane is significantly larger than its components. The signals due to the metallocycle and the fraction of macrocycle **11** forming part of the catenane showed the same diffusion coefficients, indicating that these components diffuse as a whole. In contrast, the excess of free **11** displayed a diffusion coefficient significantly larger than that of **12**·$6PF_6$ (see the Supporting Information).

Single crystals of catenane **12**·$6PF_6$ suitable for X-ray crystallography were obtained by slow diffusion of ethyl ether (4−5 days) into a solution of metallocycles **5a**,**6a**·$6PF_6$ and **11** (10 equiv) in acetonitrile. The crystal structure shows the hexacationic metallocycle **5a** interlocked by two molecules of cyclophane **11** with two parallel $\pi\cdots\pi$ stacking dispositions of three aromatic systems: HQ_{out}/PYET/HQ_{in}, where PYET, HQ_{out}, and HQ_{in} stand for the di(pyridin-4-yl)ethene unit and the alongside and inside hydroquinol rings, respectively (Figure 6). As a consequence, the di(pyridin-4-yl)ethene systems are coplanar, while the 4-phenylpyridine moiety has a torsion angle of 33°. The interplanar separation $HQ_{in}-HQ_{in}$ is 3.75 Å, and the distance between their centroids is 6.20 Å; hence one HQ_{in} is displaced 4.94 Å with respect to the other, disrupting the $HQ_{in}-HQ_{in}$ $\pi\cdots\pi$ interaction. In addition to the typical [C−H···O] bonds[21] established between the α-CH bipyridine hydrogens and the

(20) Blanco, V.; Abella, D.; Pía, E.; Platas-Iglesias, C.; Peinador, C.; Quintela, J. M. *Inorg. Chem.* **2009**, *48*, 4098.

(21) See for example: (a) Ashton, P. R.; Ballardini, R.; Balzani, V.; Credi, A.; Gandolfi, M. T.; Menzer, S.; Perezgarcia, L.; Prodi, L.; Stoddart, J. F.; Venturi, M.; White, A. J. P.; Williams, D. J. *J. Am. Chem. Soc.* **1995**, *117*, 11171. (b) Asakawa, M.; Ashton, P. R.; Balzani, V.; Brown, C. L.; Credi, A.; Matthews, O. A.; Newton, S. P.; Raymo, F. M.; Shipway, A. N.; Spencer, N.; Quick, A.; Stoddart, J. F.; White, A. J. P.; Williams, D. J. *Chem.—Eur. J.* **1999**, *5*, 860.

oxygen atoms of **11**, [N−H···O] hydrogen bonds between amine protons and the oxygen atoms of the polyether chain are also detected.[22] The dimensions of the metallocycle are 18.10×14.92 Å (palladium−palladium and methylene−methylene distances, respectively).

Experimental Section

1,1′-Methylenebis(4-((*E*)-2-(pyridin-4-yl)vinyl))pyridinium Bis(hexafluorophosphate) (1·2PF$_6$). A solution of *trans*-1,2-bis(4-pyridyl)ethylene (2.00 g, 10.9 mmol) and CH_2Br_2 (0.77 mL, 10.9 mmol) in CH_3CN (100 mL) was refluxed for 48 h. After being cooled to room temperature, the yellow precipitate was washed with CH_3CN and diethyl ether to afford a solid, which was dissolved in water (400 mL). An excess of KPF_6 was added to the solution until no further precipitation was observed. The gray solid was filtered and washed with water to afford **1**·2PF$_6$ (1.70 g, 50%). Mp 195−198 °C dec; ^{1}H NMR (500 MHz, CD_3CN) δ 6.84 (2H, s), 7.61 (2H, d, J = 16.0 Hz), 7.61 (4H, d, J = 6.5 Hz), 7.88 (2H, d, J = 16.0 Hz), 8.25 (4H, d, J = 7.0 Hz), 8.70 (4H, d, J = 6.5 Hz), 8.84 (4H, d, J = 7.0 Hz); ^{13}C NMR (125 MHz, CD_3CN) δ 77.5 (CH_2), 122.9 (CH), 126.8 (CH), 127.8 (CH), 142.4 (CH), 142.8 (C), 145.8 (CH), 151.7 (CH), 157.6 (C); MS-ESI (m/z) 523.15 [M − PF$_6^-$]$^+$, 377.17 [M − H$^+$ − 2PF$_6^-$]$^+$, 189.09 [M − 2PF$_6^-$]$^{2+}$. Anal. Calcd for $C_{25}H_{22}F_{12}N_4P_2$: C, 44.92; H, 3.32; N, 8.38. Found: C, 45.17; H, 3.09; N, 8.52.

1,1′-Methylenebis(4-((*E*)-2-(pyridin-4-yl)vinyl))pyridinium Bis(nitrate) (1·2NO$_3$). To a solution of ligand **1**·2PF$_6$ (0.62 g, 0.93 mmol) in CH_3CN (100 mL) was added an excess of Bu_4NNO_3 until no further precipitation is observed. The red precipitate was filtered and washed with CH_3CN to yield **1**·2NO$_3$ (0.39 g, 83%). Mp 178−180 °C dec; ^{1}H NMR (500 MHz, CD_3CN) δ 7.27 (2H, s), 7.68 (2H, d, J = 16.4 Hz), 7.76 (4H, d, J = 5.6 Hz), 7.93 (2H, d, J = 16.4 Hz), 8.36 (4H, d, J = 6.8 Hz), 8.64 (4H, d, J = 6.0 Hz), 9.16 (4H, d, J = 6.8 Hz); ^{13}C NMR (125 MHz, CD_3CN) δ 76.8 (CH_2), 122.8 (CH), 126.0 (CH), 127.8 (CH), 140.3 (CH), 143.7 (C), 144.5 (CH), 148.8 (CH), 156.5 (CH), 156.3 (C); MS-ESI (m/z) 189.09 [M − 2NO$_3^-$]$^{2+}$. Anal. Calcd for $C_{25}H_{22}N_6O_6$: C, 59.76; H, 4.41; N, 16.73. Found: C, 59.51; H, 4.22; N, 16.98.

(*E*)-1-(4-(Pyridin-4-yl)benzyl)-4-(2-(pyridin-4-yl)vinyl)pyridinium Hexafluorophosphate (2·PF$_6$). A solution of 4-(4′-chloromethylphenyl)pyridine (0.84 g, 4.12 mmol) cooled to 0 °C in CH_3CN (50 mL) was slowly added to a solution of *trans*-1,2-bis(4-pyridyl)-ethylene (3.00 g, 16.46 mmol) and a catalytic amount of KI in refluxing CH_3CN (70 mL). The reaction was refluxed for 24 h; after cooling, the solvent was evaporated in vacuo. The resulting residue was triturated with ethyl ether (6 × 100 mL) to give a crude product, which was purified by column chromatography (SiO_2, acetone/NH_4Cl 1.5 M/MeOH 5:4:1). The product-containing fractions were combined and the solvents were removed in vacuo. The residue was dissolved in H_2O/CH_3OH (95/5, 900 mL) and an excess of KPF_6 was added until no further precipitation was observed. The solid was filtered and washed with water to give **2**·PF$_6$ (0.33 g, 16%) as a white solid. Mp 214−216 °C dec; ^{1}H NMR (500 MHz, CD_3CN) δ 5.76 (2H, s), 7.63 (2H, d, J = 8.5 Hz), 7.67 (1H, d, J = 16.5 Hz), 7.78−7.81 (3H, m), 7.93 (2H, d, J = 8.4 Hz), 8.04 (2H, d, J = 6.7 Hz), 8.15 (2H, d, J = 6.9 Hz), 8.69 (4H, m), 8.72 (2H, d, J = 6.9 Hz); ^{13}C NMR (125 MHz, CD_3CN) δ 64.1 (CH_2), 123.9 (CH), 124.6 (CH), 126.6 (CH), 129.7 (CH), 130.3 (CH), 131.0 (CH), 136.9 (C), 137.9 (C), 138.5 (CH), 145.6 (CH), 145.8 (CH), 146.6 (C), 148.7 (CH), 153.9 (C), 154.4 (C); MS-ESI (m/z) 350.4 [M − PF$_6^-$]$^+$. Anal. Calcd for $C_{24}H_{20}F_6N_3P$: C, 58.19; H, 4.07; N, 8.48. Found: C, 58.38; H, 4.30; N, 8.44.

(22) Distances: [H···O] 2.20 Å, and [N···O] 3.06 Å. Angle: [N−H···O], and 156°.

(*E*)-1-(4-(Pyridin-4-yl)benzyl)-4-(2-(pyridin-4-yl)vinyl)pyridinium Nitrate (2·NO$_3$). Ligand **2**·PF$_6$ (100.0 mg, 0.20 mmol) was dissolved in CH_3CN and an excess of Bu_4NNO_3 was added until no further precipitation is observed. The white precipitate was filtered and washed with CH_3CN to yield **2**·NO$_3$ (60.4 mg, 73%). Mp 166−168 °C dec; ^{1}H NMR (500 MHz, D_2O) δ 5.82 (2H, s), 7.61 (2H, d, J = 8.3 Hz), 7.61 (1H, d, J = 16.3 Hz), 7.75−7.78 (3H, m), 7.90 (2H, d, J = 8.3 Hz), 7.95 (2H, d, J = 6.3 Hz), 8.16 (2H, d, J = 6.8 Hz), 8.60 (2H, d, J = 6.3 Hz), 8.64 (2H, d, J = 6.6 Hz), 8.83 (2H, d, J = 6.8 Hz); ^{13}C NMR (125 MHz, CD_3CN) δ 63.2 (CH_2), 122.9 (CH), 123.1 (CH), 125.3 (CH), 128.4 (CH), 128.7 (CH), 129.7 (CH), 135.0 (C), 137.4 (CH), 137.5 (C), 144.2 (CH), 145.0 (C), 145.8 (CH), 147.9 (CH), 151.8 (C), 152.9 (C); MS-ESI (m/z) 350.2 [M − NO$_3^-$]$^+$. Anal. Calcd for $C_{24}H_{20}N_4O_3$: C, 69.89; H, 4.89; N, 13.58. Found: C, 70.18; H, 4.63; N, 13.34.

Metallocycle 4a·8NO$_3$. To a solution of **1**·2NO$_3$ (4.0 mg, 8.0×10^{-3}mmol) in D_2O (4.0 mL) was added (en)Pd(NO$_3$)$_2$ (**3b**) (2.3 mg, 8.0×10^{-3}mmol). ^{1}H NMR (500 MHz, D_2O) δ 2.91 (8H, br s), 7.27 (4H, s), 7.61 (4H, d, J = 16.4 Hz), 7.74−7.78 (12H, m), 8.27 (8H, d, J = 7.0 Hz), 8.78 (8H, d, J = 6.8 Hz), 9.17 (8H, d, J = 7.0 Hz); ^{13}C NMR (125 MHz, D_2O) δ 46.6 (CH_2), 77.1 (CH_2), 124.9 (CH), 126.3 (CH), 129.8 (CH), 137.8 (CH), 144.6 (CH), 145.8 (C), 151.4 (CH), 155.6 (C).

Metallocycle 4a·4OTf·4PF$_6$. To a solution of **1**·2PF$_6$ (20.1 mg, 0.030 mmol) in CD_3CN (3.0 mL) was added (en)Pd(OTf)$_2$ (**3a**) (15.3 mg, 0.033 mmol). ^{1}H NMR (500 MHz, CD_3CN) δ 2.83 (8H, br s), 4.25 (8H, s), 6.89 (4H, s), 7.58 (4H, d, J = 16.5 Hz), 7.70−7.73 (12H, m), 8.17 (8H, d, J = 7.0 Hz), 8.78 (8H, d, J = 6.8 Hz), 8.91 (8H, d, J = 7.1 Hz); ^{13}C NMR (125 MHz, CD_3CN) δ 47.7 (CH_2), 77.7 (CH_2), 125.7 (CH), 127.4 (CH), 131.0 (CH), 138.7 (CH), 146.0 (CH), 146.7 (C), 153.1 (CH), 156.3 (C).

Metallocycle 4b·8PF$_6$. A solution of ligand **1**·2PF$_6$ (100.3 mg, 0.150 mmol) and (en)Pt(OTf)$_2$ (**3c**) (91.3 mg, 0.165 mmol) in CH_3CN (15 mL) was heated at 70 °C for 5 d. The solvent was removed under reduced pressure without heating. The crude product was suspended in water and ion-exchange resin (0.50 g) was added. The mixture was stirred at room temperature for 24 h. The resin was removed by filtration and an excess of KPF_6 is added to the filtrate until no further precipitation was observed. The solid was filtered and washed with water to yield **4b**·8PF$_6$ as a pink solid (236.8 mg, 65%). Mp 251−253 dec; ^{1}H NMR (500 MHz, CD_3CN) δ 2.76 (8H, br s), 4.79 (8H, s), 6.87 (4H, s), 7.61 (4H, d, J = 16.4 Hz), 7.70 (8H, d, J = 6.8 Hz), 7.73 (4H, d, J = 16.5 Hz), 8.19 (8H, d, J = 6.9 Hz), 8.75 (8H, d, J = 6.8 Hz), 8.86 (8H, d, J = 7.0 Hz); ^{13}C NMR (125 MHz, CD_3CN) δ 48.6 (CH_2), 77.8 (CH_2), 126.1 (CH), 127.4 (CH), 131.1 (CH), 138.5 (CH), 145.9 (CH), 146.7 (C), 153.8 (CH), 156.3 (C). HRMS-ESI (m/z) calcd for [M − 3PF$_6^-$]$^{3+}$ 663.7517, found 663.7522; calcd for [M − 4PF$_6^-$]$^{4+}$ 461.5726, found 461.5746; calcd for [M − 5PF$_6^-$]$^{5+}$ 340.2651, found 340.2656. Anal. Calcd for $C_{54}H_{60}F_{48}N_{12}P_8Pt_2$: C, 26.72; H, 2.49; N, 6.93. Found: C, 26.50; H, 2.66; N, 7.21.

Metallocycle 4b·8NO$_3$. To a solution of **4b**·8PF$_6$ (60.0 mg, 0.025 mmol) in CH_3CN (10 mL) was added an excess of Bu_4NNO_3 until no further precipitation is observed. The red precipitate is filtered and washed with CH_3CN to yield **4b**·8NO$_3$ (35 mg, 82%). ^{1}H NMR (500 MHz, D_2O) δ 2.82 (8H, s), 7.17 (4H, s), 7.53 (4H, d, J = 16.5 Hz), 7.62 (8H, d, J = 6.5 Hz), 7.67 (4H, d, J = 16.0 Hz), 8.18 (8H, d, J = 7.0 Hz), 8.70 (8H, d, J = 6.5 Hz), 9.07 (8H, d, J = 7.0 Hz); ^{13}C NMR (125 MHz, D_2O) δ 47.4 (CH_2), 77.1 (CH_2), 125.3 (CH), 126.3 (CH), 129.8 (CH), 137.6 (CH), 144.6 (CH), 145.7 (C), 152.1 (CH), 155.5 (C). Anal. Calcd for $C_{54}H_{60}N_{20}O_{24}Pt_2$: C, 36.78; H, 3.43; N, 15.89. Found: C, 36.49; H, 3.17; N, 15.97.

Catenane 12·6PF$_6$. To a solution of **5a**,**6a**·6PF$_6$ (5.7 mg, 0.003 mmol) in CD_3CN (0.6 mL) was added **11** (32.2 mg, 0.060 mmol). ^{1}H NMR (500 MHz, CD_3CN) δ 2.88 (8H, s), 2.96−3.00 (12H, m), 3.15 (8H, m), 3.34−3.36 (12H, m), 3.60 (m,

excess of **11**), 3.74 (m, excess of **11**), 3.96 (m, excess of **11**), 4.35 (4H, br s), 4.47 (4H, br s), 5.58 (4H, s), 5.71 (16H, s), 6.32 (2H, d, J = 16.3 Hz), 6.42 (2H, d, J = 16.3 Hz), 6.75 (s, excess of **11**), 7.00 (4H, d, J = 6.5 Hz), 7.50 (4H, d, J = 6.6 Hz), 7.58 (4H, d, J = 8.4 Hz), 7.68 (4H, d, J = 8.4 Hz), 7.78 (4H, d, J = 6.8 Hz), 8.68 (4H, d, J = 6.4 Hz), 8.71 (4H, d, J = 6.6 Hz), 8.86 (4H, d, J = 6.8 Hz); ^{13}C NMR (125 MHz, CD_3CN) δ 47.9 (CH_2), 64.1 (CH_2), 67.6 (CH_2), 68.7 (CH_2, excess of **11**), 70.3 (CH_2), 70.4 (CH_2, excess of **11**), 70.9 (CH_2), 71.2 (CH_2, excess of **11**), 71.2 (CH_2, excess of **11**), 114.9 (CH), 116.1 (CH, excess of **11**), 124.9 (CH), 125.4 (CH), 126.4 (CH), 128.6 (CH), 129.1 (CH), 130.9 (CH), 133.9 (CH), 137.5 (C), 137.5 (C), 145.8 (CH), 146.3 (C), 151.5 (C), 151.8 (C), 152.6 (CH), 152.8 (C), 153.2 (CH), 153.9 (C, excess of **11**).

Single crystals of the catenane **12**·6PF_6 suitable for X-ray diffraction were obtained by slow diffusion of ethyl ether into a solution of **5a**,**6a**·6PF_6 and **11** in acetonitrile.

Acknowledgment. The authors thank Centro de Supercomputación de Galicia for providing the computer facilities. This research was supported by Xunta de Galicia (PGIDIT06PXIB103224PR), Ministerio de Educación y Cultura, and FEDER (CTQ2007-63839/BQU). V.B. and A.G. thank the Ministerio de Educación y Ciencia (FPU Program) and the Universitat de Barcelona for their predoctoral fellowships.

Supporting Information Available: ^{1}H NMR, ^{13}C NMR, and 2D experiments for all compounds, crystallographic files (in CIF format) of metallocycle **4a**·4OTf·4PF_6 and catenane **12**·6PF_6, titrations data, and optimized Cartesian coordinates (BH&H/6-31+G(d) level) for **5a** and **6a**. This material is available free of charge via the Internet at http://pubs.acs.org.